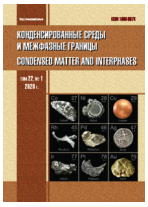

Condensed Matter and Interphases
(Kondensirovannye sredy i mezhfaznye granitsy)

Original articles

DOI: https://doi.org/10.17308/kcmf.2020.22/2821
Received 12 Mach 2020
Accepted April 2020
Published online 25 June 2020

ISSN 1606-867X
eISSN 2687-0711

Synthesis and Properties of Synthetic Aikinite $PbCuBiS_3$

© 2020 O. M. Aliev[a], S. T. Bayramova[b], D. S. Azhdarova[a], Sh. H. Mammadov[a]✉, V. M. Ragimova[a], T. F. Maksudova[b]

[a]*M. Nagiyev Institute of Catalysis and Inorganic Chemistry of National Academy of Sciences of Azerbaijan, 113 G. Javid ave., Baku AZ 1143, Azerbaijan*

[b]*Baku European Lyceum, 37 Rostropovich str., Baku AZ 1001, Azerbaijan*

Abstract

The goal of this study was the synthesis and study of the properties of synthetic aikinite, $PbCuBiS_3$.

The synthesis was carried out in evacuated quartz ampoules for 7–8 h; the maximum temperature was 1250–1325 K. Next, the samples were cooled and kept at 600 K for a week. Then the ampoules were opened, the samples were carefully ground, and after melting, annealed at 600–800 K, depending on the composition, for at least two weeks to bring the samples into equilibrium. The annealed samples were studied by differential thermal (DTA), X-ray diffraction (XRD), microstructural (MSA) analyses, as well as microhardness measurements and density determination. XRD was performed using D 2 PHASER with CuK_α radiation and a Ni filter.

$CuBiS_2$–PbS, Cu_2S–$PbCuBiS_3$, Bi_2S_3–$PbCuBiS_3$, $PbBi_2S_4$–$PbCuBiS_3$, $PbBi_4S_7$–$PbCuBiS_3$ sections of quasi-triple system Cu_2S–Bi_2S_3–PbS were studied using the complex of physical and chemical analysis methods and their phase diagrams were plotted. It was found that in addition to the $PbBi_2S_4$–$PbCuBiS_3$ section, all sections are quasi-binary and they were characterized by the presence of limited solubility regions based on the initial components. The study of the $CuBiS_2$-PbS section revealed the formation of a quaternary compound $PbCuBiS_3$ occurring in nature as the mineral aikinite, congruently melting at 980 K. We established that $PbCuBiS_3$ crystallizes in a rhombic syngony with lattice parameters a = 1.1632, b = 1.166, c = 0.401 nm, Pnma space group, Z = 4. Using DTA and XRD methods we established that $PbCuBiS_3$ compound is a phase of variable composition with a homogeneity range from 45 to 52 mol%/PbS. The $PbCuBiS_3$ compound is a p-type semiconductor with a band gap energy of ΔE = 0.84 eV.

Keywords: aikinite, compound, single crystal, structure, thermodynamic function, band gap energy.

For citation: Aliev O. M., Bayramova S. T., Azhdarova D. S., Mammadov Sh. H., Ragimova V. M., Maksudova T. F. Synthesis and Properties of Synthetic Aikinite $PbCuBiS_3$. *Kondensirovannye sredy i mezhfaznye granitsy = Condensed Matter and Interphases.* 2020; 22(2): 182–189. DOI: https://doi.org/10.17308/kcmf.2020.22/2821

1. Introduction

Minerals possess specific semiconductor, optical, and electro-optical properties, allowing them to be used as semiconductors in special devices. All this determines the attention paid to the synthesis of aikinite and the growth of aikinite single crystals.

Now one of the most promising materials of modern electronics are chalcogenide phases of the A_2B_3 type. Physicochemical and electrophysical parameters of these materials are easily controllable and have a wide spectrum of action. A_2B_3 type (A = Sb, Bi; B = S, Se, Te) chalcogenides possess thermoelectric and photoelectric properties. These features of thematerials create favourable conditions for their widespread use in the electronics industry [1–7]

Compound $PbCuBiS_3$ occurs in nature in the form of a mineral and crystallizes in rhombic syngony with a lattice period: a = 1.1632, b = 1.166, c = 0.401 nm, Pnma space group, Z = 4 [8–18]. The structure is similar to the structure of antimonite K_2CuCl_2 and others [3] and similar to the structure of

✉ Sharafat H. Mammadov, e-mail: azxim@mail.ru

bournonite $PbCuSbS_3$ and zeligmannite $PbCuAsS_3$. The exact distribution of Pb and Bi atoms in the crystal lattice has not been elucidated. In comparison with Bi_2S_3 in aikinite replacement of Bi^{+3} with Pb^{+2} compensated by the inclusion of a single Cu^+ ion of such small size that it occupies the empty spaces of the lattice without distorting it.

The lead atoms in the aikinite structure are surrounded by five sulphur atoms with distances from 0.284 to 0.298 nm and two more sulphur atoms separated by 0.324 nm, and the coordination is close to octahedral (Fig. 1).

Extensive experimental studies of natural minerals showed that all the considered compounds are ordered, their compositions are limited to a certain stoichiometry and very narrow regions of solid solutions, as was previously assumed in [19]. According to available data, the structure of all these minerals is a derivative of the structure of bismuthine, obtained by substitution of Bi in the latter with Pb with the simultaneous addition of Cu atoms to the vacant tetrahedral sites Cu + Pb + Bi [8, 9]. There are three types of ribbons in the structures of these minerals [9], the combination of which can lead to the motives of all the minerals of this series: bismuthine Bi_4S_6, krupkaite $CuPbBi_3S_6$, and aikinite.

It should be noted that although the ratio between metal sulphides is Cu_2S:PbS in the aikinite–bismuthine series is constant and equal to 1:2, in a selenium-containing mineral of a similar composition $Cu_2Pb_3Bi_8(S, Se)_{16}$ it is 1:3, which also exhibited as slightly altered arrangement of atoms. The basis of the structural motif is composed by zigzag ribbons of Pb and Bi octahedra connected along the edges, linked together by pairs of other octahedrons also with an edge bonds. In the voids of this structure, additional Pb and Bi atoms are located in seven-dimensional coordination. The environment of Cu atoms is intermediate between tetrahedral and plane triangular, the Cu–S distances are 232 nm (3 S) and 252 nm (1 S) [13, 17].

Earlier, we [20, 25] synthesized and studied the physicochemical and physical properties of complex sulfosalts based on the $PbCuSbS_3$ bournonite mineral.

The purpose of this work was the synthesis and study of the properties of synthetic aikinite $PbCuBiS_3$.

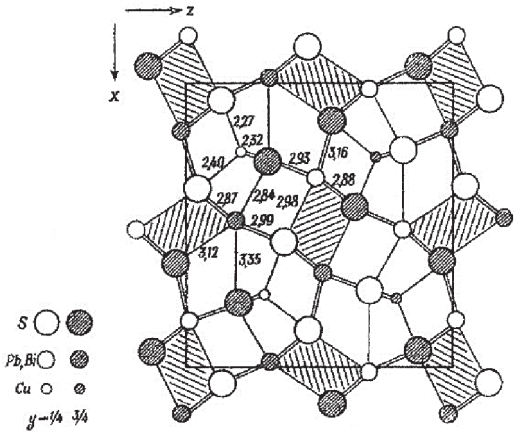

Fig. 1. The crystal structure of the aikinite mineral $PbCuBiS_3$ [1]

2. Experimental

Quaternary sulfosalt $PbCuBiS_3$ was revealed while studying the $CuBiS_2$–PbS section of the quasi-triple Cu_2S–Bi_2S_3–PbS system. The quasi-triple system, except for $CuBiS_2$–PbS, was studied by based on Cu_3BiS_3–$PbCuBiS_3$, $CuBi_3S_5$–$PbCuBiS_3$, Cu_2S–$PbCuBiS_3$, $PbBi_2S_4$–$PbCuBiS_3$, $PbBi_4S_7$–$PbCuBiS_3$ and Bi_2S_3–$PbCuBiS_3$ sections. The position of the connodes in the Cu_2S–Bi_2S_3–PbS system is shown in Fig. 2.

The quaternary alloys for the study were obtained by the vacuum-thermal method from the source alloys ($CuBiS_2$, PbS, $CuBi_2S_4$ etc.), previously synthesized from ultra-pure elements (Cu – 99.997 %, Pb – 99.994 wt%, Bi – 99.999 wt%, S – 99.9999 wt%). The maximum temperature was 1250–1325 K. The synthesis was carried out in evacuated quartz ampoules for 7–8 h; then, the samples were cooled and kept at 600 K for a week [26]. Then the ampoules were opened, the samples were carefully ground, and after melting, annealed at 600–800 K, depending on the composition, for at least two weeks to bring the samples into equilibrium, Table 1.

Annealed samples were studied by physicochemical analysis: thermal analysis was carried out using Kurnakov pyrometer NTR-73 (heating rate 10 °/min, standard Al_2O_3, chromel-alumel thermocouple); XRD patterns were obtained using D 2 PHASER Brucker diffractometer (CuK_α-radiation, Ni-filter); the microhardness of the samples was measured using PMT-3 microhardness tester (optimal load of 0.02 kg), the microstructure of the alloys

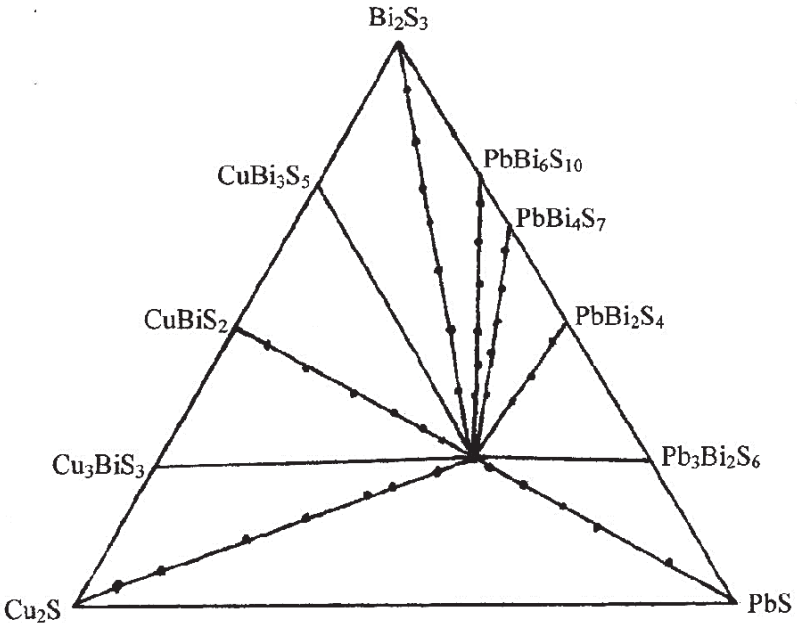

Fig. 2. The position of the connodes in the PbS–Cu_2S–Bi_2S_3 system. The compositions of the synthesized samples are indicated by black dots

Table 1. Results of physicochemical analysis of alloys of the $CuSbS_2$–PbS system

Composition, mol% PbS	Thermal effects, K		Microhardness ($x10^7$ Pa)	Density, g/cm^3	Phase composition
	solidus	liquidus			
0.0	-	780	2200	7.40	$CuBiS_2$ (single phase)
5.0	715	765	2250	7.38	α
10	650	730	2300	7.32	α+β
15	650	690	2300	7.30	α+β
20	650	700	eutectic	7.28	α+β
25	650	765	-	7.28	α+β
30	650	830	1980	7.26	α+β
40	650	925	1980	7.24	α+β
45	-	970	1970	7.22	β
50	-	980	1980	7.20	β
52	-	970	1990	-	β
55	815	930	1990	-	β + PbS
60	810	865	-	7.12	β+ PbS
65	815	-	eutectic	7.06	β+ PbS
70	815	920	720	6.90	β+ PbS
80	815	1070	720	6.82	β+ PbS
90	815	1240	720	6.70	β+ PbS
100	-	1400	720	6.11	Pbs (single phase)

was studied using a MIM-7 microscope, and the density was determined by the pycnometer.

3. Results and discussion

We will discuss in details the $CuSbS_2$–PbS system, in which the sulfosalt $PbCuBiS_3$ was found.

As can be seen from Table 1, the microhardness value related to the $PbCuBiS_3$ quaternary compound, increased on both sides from 50 mol% PbS, but it decreased with stoichiometric composition. This shows that a range of homogeneity exists based on the $PbCuBiS_3$ compound. According to the results of XRD and microstructural analysis, it

was found that $PbCuBiS_3$ is a phase of variable composition and that solubility at a eutectic temperature (650 K) was 10 mol%, while with decreasing temperature it sharply narrows, not exceeding 7 mol% PbS at 300 K.

The MSA analysis showed that with the exception of compositions 0–7 and 45–52 mol% PbS, all alloys were biphasic.

According to the physicochemical analysis, a phase diagram of the $CuBiS_2$–PbS system was plotted and it is shown in Fig. 3. As can be seen from the figure, the system is characterized by the presence of $PbCuBiS_3$ sulfosalt melting at 980 K congruently. Coordinates of eutectic points: 20 mol% PbS 650 K, and 65 mol% PbS 815 K. XRD demonstrated that in the range of concentrations of 0–7 mol% PbS, only reflections related to $CuBiS_2$ were observed on diffractograms. These solutions crystallize in rhombic syngony, and with an increase in the concentration of PbS, the lattice parameters increase (a = 0.614÷0.620, b = 0.391÷0.395, c = 1.493÷1.502 nm, Pnma space group, Z = 4).

In the range of concentration 7÷45 mol% PbS α-solid solutions based on $CuBiS_2$ and β-solid solutions based on quaternary sulfosalt $PbCuBiS_3$ co-crystallize and in the 52÷100 mol% PbS two phases (β + PbS) co-crystallize. Composition 50 mol% PbS in terms of interplanar spacing and intensity differed from the source sulphides. Calculation of XRD patterns of the quaternary compound $PbCuBiS_3$, as well as XRD patterns of the initial sulphides for comparison are presented in Table 2.

X-ray analysis confirmed the formation of quaternary sulfosalts $PbCuBiS_3$, found in nature in the form of the mineral aikinite in $CuBiS_2$–PbS system. It was found that sulfosalt crystallizes in rhombic syngony with unit cell parameters a = 1.1632, b = 1.166, c = 0.4017 nm, Pnma space group, Z = 4.

The Bi_2S_3-$PbCuBiS_3$ section is of eutectic type. The composition of the eutectic point determined by the plotting of the Tamman's triangle was 50 mol% Bi_2S_3 at 800 K. Solubility based on Bi_2S_3 was 5 mol%, based on $PbCuBiS_3$ – 7 mol% (Fig. 4a).

The Cu_2S – $PbCuBiS_3$ section was quasi-binary and eutectic with limited solubility based on the starting sulphides (Fig. 4b).

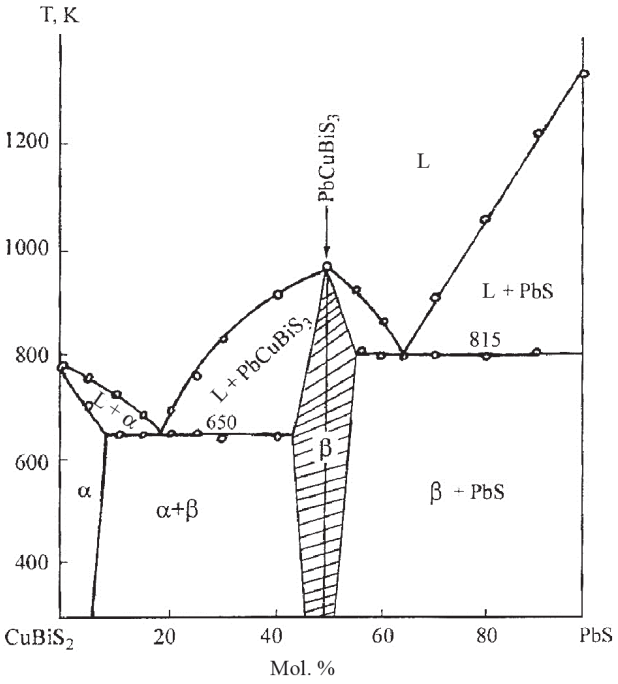

Fig. 3. Phase diagram of the $CuBiS_2$-PbS system

Conclusion on the formation of solid solutions based on α-, β- and γ-Cu_2S was based on the results of the DTA and MSA methods. On thermograms of samples containing 7 and 8 mol % $PbCuBiS_3$, thermal effects below the solidus temperature were revealed. These effects were associated with the formation and decomposition of a solid solution based on γ-Cu_2S. This was also confirmed by the MSA data. In samples containing from 2 to 5.5 mol% $PbCuBiS_3$, the second phase was present in the form of needle insertions, and eutectic was not revealed. In the Cu_2S–$PbCuBiS_3$ system in the range of concentrations of 2.0–90 mol% $PbCuBiS_3$ in a condensed state, two phases were in equilibrium: αCu_2S-based solid solution and β-$PbCuBiS_3$ based solid solution. They were clearly distinguishable by MSA and formed a eutectic of the composition 40 mol % Cu_2S and T = 850 K. Eutectic in the indicated concentration range was present on the sections of all section samples and it was represented by the alternation of needle crystals of the $PbCuBiS_3$ phase and oval Cu_2S crystals. Based on α-Cu_2S a limited solution was formed, which at 300 K reached 2 mol% $PbCuBiS_3$.

The phase transitions α-Cu_2S ↔ β-Cu_2S ↔ γ-Cu_2S had a eutectic nature and occurred at 375 and 580 K, respectively. Thermal effects related to β-Cu_2S↔ γ-Cu_2S were revealed only for alloys

Table. 2. Interplanar distances and intensities of the $CuBiS_2$, $PbCuBiS_3$ and PbS lines for comparison

$CuBiS_2$		$PbCuBiS_3$			PbS	
d_{exp}, E	I/I_0	d_{exp}, Å	I/I_0	*hkl*	d_{exp}, Å	I/I_0
4.700	8	4.070	4	220	3.790	2
3.200	10	3.770	1	011	3.442	9
3.100	8	3.670	10	130	3.283	3
3.020	10	3.580	7	111, 310	2.965	10
2.810	2	3.180	9	121	2.311	2
2.340	9	2.880	8	040, 221	2.693	10
2.290	4	2.740	2	410	1.780	9
2.160	9	2.680	3	131, 330	1.707	8
1.960	5	2.620	6	311	1.480	5
1.880	7	2.580	1	240	1.359	6
1.800	8	2.560	1	420	1.324	10
1.780	3	2.510	3	231	1.209	8
1.755	3	2.570	2	150	1.141	7
1.655	8	2.170	3	241	1.048	3
1.560	5	2.150	3	250, 421		
1.475	2	2.020	5	440, 051		
1.450	4	1.984	4	431, 151		
1.365	3	1.974	3	530, 112		
1.320	4	1.883	1	202, 600		
1.260	2	1.805	4	441		
1.125	5	1.766	1	351, 133		
1.208	5	1.648	4	042, 170		
1.190	5	1.593	4	270		
1.168	7	1.514	1	370		
1.112	3	1.475	2	171		
1.100	3	1.406	4	740		
		1.380	2	561		
		1.354	2	612		
		1.330	3	003		
		1.278	2	661		
		1.158	1	770		

containing 10÷20 mol% $PbCuBiS_3$, therefore, this transition in Fig. 4b was marked with a dotted line.

The $PbBi_2S_4$–$PbCuBiS_3$ section was partially quasi-binary due to the incongruent nature of the melting of sulphide $PbBi_2S_4$. The solubility based on $PbCuBiS_3$ sulfosalt was 8 mol% at 300 K, and at a eutectic temperature of 15 mol% Coordinates of the eutectic point were 40 mol% $PbCuBiS_3$ and T = 825 K.

The $PbBi_4S_7$–$PbCuBiS_3$ section was quasi-binary and eutectic with limited solid solutions. The eutectic corresponds to 55 mol% $PbBi_4S_7$ and 800 K. The solubility of $PbCuBiS_3$ in $PbBi_4S_7$ at eutectic temperature was 10 mol%, at 300 K it decreased to 5 mol% $PbCuBiS_3$ (α-solid solution), and the solubility of $PbBi_4S_7$ in quaternary sulphide was 18 mol% at eutectic temperature and decreased to 10 mol% $PbBi_4S_7$ at 300 K β-solid solution).

$PbCuBiS_3$ single crystals were obtained by targeted crystallization of a stoichiometric melt in vertical quartz ampoules. An ampoule with a cone-shaped bottom was placed in a furnace with a small temperature gradient in height. After the formation of the melt, directed cooling was carried out at a speed of 4 °/h for 48 h until the entire melt solidified, then the furnace was cooled at a speed of 60 °/h. Thus, polycrystalline ingots with a large number of cracks were obtained.

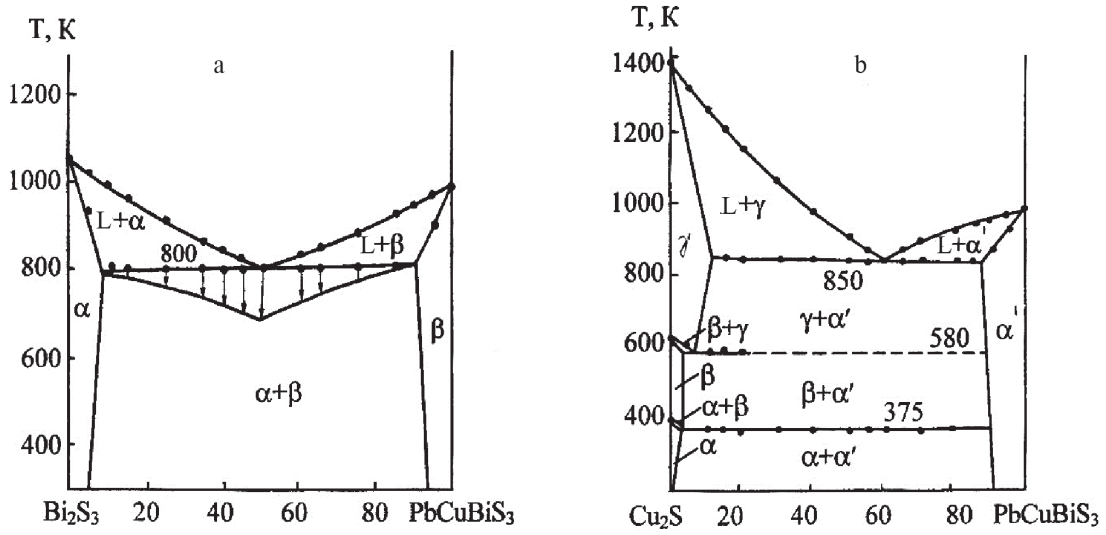

Fig. 4. Phase diagram of the Bi_2S_3–$PbCuBiS_3$ (a) and Cu_2S–$PbCuBiS_3$ (b) systems

However, it was possible to cut single crystal sections with a length of 1 mm, free of visible defects from these ingots (Fig. 5).

Significantly larger single crystals of the $PbCuBiS_3$ compound were obtained by the similar method in quartz ampoules with a diameter of 5 mm. The single crystals reached a length of 8–12 mm with a diameter of 5 mm. One feature of the $PbCuBiS_3$ compound should be noted: directional crystallization of stoichiometric composition without special additives always provided ingots characterized mainly by p-type conductivity. It is possible that this was the result of a deviation from stoichiometry due to the combination of volatile components (sulphur and bismuth). The ingot always contained an excess of copper, which in significant quantities dissolves in the compound and provides *p*-type conductivity. Therefore, any doping of the $PbCuBiS_3$ compound (obtained $PbCuBiS_3$ crystals were doped with erbium) during crystal growth by directed cooling will occur against the background of this phenomenon.

The standard thermodynamic functions of the $PbCuBiS_3$ compound were calculated: S^0_{298} = 253.1±5 J/(mol%), ΔS^0_{298} = −14.1±3 J/mol, ΔH^0_{298} = −270.2±10 kJ/mol and ΔG^0_{298} = −266.3±10 kJ/mol

The photoconductivity spectra of pure $PbCuBiS_3$ crystals and crystals doped with erbium grown by the directed crystallization method from the melt were studied. The spectral dependences of these sulfosalts are shown in Fig. 6. As can be seen, crystals grown by directional crystallization had approximately the same photosensitivity, which at 293 K was $I_{St}/I_t = 10^3$ when illuminated by natural light, and when the temperature decreased, it grew and reached 10^5 at 100 K. In

Fig. 5. Single crystals of the $PbCuBiS_3$ compound

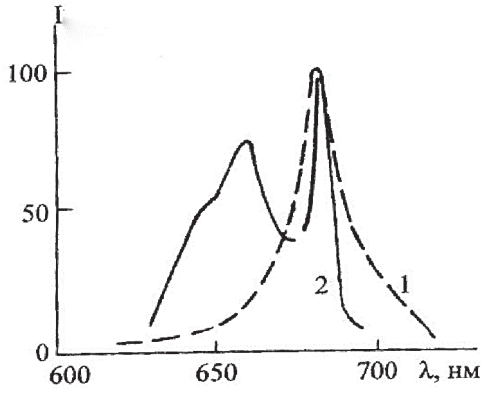

Fig. 6. The spectral dependence of the photoconductivity of $PbCuBiS_3$ (*1*) and $PbCuBiS_3$–Er (*2*) grown by the directed crystallization method

crystals of both types, bands of shallow levels - traps with an activation energy of 0.25–0.35 eV, as well as trap levels with an activation energy ΔE = 0.50–0.60 eV, were observed. The band gap energy calculated from photoconductivity was ΔE = 0.84–0.91 eV.

Thus, the nature of the formation of $PbCuBi_3$ sulfosalt was revealed based on studying the quasi-triple $Cu_2S–Bi_2S_3–PbS$ system based on $CuBiS_2–PbS$, $Cu_2S–PbCuBiS_3$, $PbBi_2S_4–PbCuBiS_3$, $PbBi_4S_7–PbCuBiS_3$ and $Bi_2S_3–PbCuBiS_3$ sections. The single crystals of synthetic aikinite $PbCuBiS_3$ were grown and some of its properties were studied.

4. Conclusions

1. The $CuBiS_2–PbS$, $Cu_2S–PbCuBiS_3$, $Bi_2S_3–PbCuBiS_3$, $PbBi_2S_4–PbCuBiS_3$, $PbBi_4S_7–PbCuBiS_3$ sections of quasi-triple $Cu_2S–Bi_2S_3–PbS$ system were studied by a set of physicochemical analysis methods and their phase diagrams were plotted. It was established that in addition to the $PbBi_2S_4–PbCuBiS_3$ section, all sections were quasi-binary and they were characterized by the presence of limited solubility regions based on the source components.

2. The study of $CuBiS_2–PbS$ section revealed the formation of a quaternary compound of the $PbCuBiS_3$ composition, found in nature in the form of the mineral aikinite, melting congruently at 980 K. It was established that $PbCuBiS_3$ crystallizes in rhombic syngony with lattice parameters a = 1.1632, b = 1.166, c = 0.401 nm, Pnma space group, Z = 4.

3. $PbCuBiS_3$ single crystals were grown by directional crystallization and the spectral dependence of photoconductivity was studied. It was established that $PbCuBiS_3$ possesses photosensitivity in the visible region of the spectrum.

Conflict of interests

The authors declare that they have no known competing financial interests or personal relationships that could have influenced the work reported in this paper.

References

1. Zhang Y-X., Ge Z-H., Feng J. Enhanced thermoelectric properties of $Cu_{1.8}S$ via introducing Bi_2S_3 and Bi_2S_3/Bi core-shell nanorods. *Journal of Alloys and Compounds*.2017;727: 1076–1082. DOI: https://doi.org/10.1016/j.jallcom.2017.08.224

2. Mahuli N., Saha D., Sarkar S. K. Atomic layer deposition of p-type Bi_2S_3. *Journal of Physical Chemistry C*. 2017;121(14): 8136–8144. DOI: https://doi.org/10.1021/acs.jpcc.6b12629

3. Ge Z-H, Qin P., He D, Chong X., Feng D., Ji Y-H., Feng J., He J. Highly enhanced thermoelectric properties of Bi/Bi_2S_3 nano composites. *ACS Applied Materials & Interfaces*. 2017;9(5): 4828–4834. DOI: https://doi.org/10.1021/acsami.6b14803

4. Savory C. N., Ganose A. M., Scanlon D. O. Exploring the $PbS–Bi_2S_3$ series for next generation energy conversion materials. *Chemistry of Materials*. 2017;29(12): 5156 – 5167. DOI: https://doi.org/10.1021/acs.chemmater.7b00628

5. Li X., Wu Y, Ying H., Xu M., Jin C., He Z., Zhang Q., Su W., Zhao S. In situ physical examination of Bi_2S_3 nanowires with a microscope. *Journal of Alloys and Compounds*. 2019;798: 628–634. DOI: https://doi.org/10.1016/j.jallcom.2019.05.319

6. Patila S. A., Hwanga Y-T., Jadhavc V. V., Kimc K. H., Kim H-S. Solution processed growth and photoelectrochemistry of Bi_2S_3 nanorods thin film. *Journal of Photochemistry & Photobiology, A: Chemistry*. 2017;332: 174–181. DOI: https://doi.org/10.1016/j.jphotochem.2016.07.037

7. Yang M., Luo Y. Z., Zeng M. G., Shen L., Lu Y. H., Zhou J., Wang S. J., Souf I. K., Feng Y. P. Pressure induced topological phase transition in layered Bi_2S_3. *Physical Chemistry Chemical Physics*.2017;19(43): 29372–29380. DOI: https://doi.org/10.1039/C7CP04583B

8. Kohatsu I., Wuensch B. J. The crystal structure of aikinite, $PbCuBiS_3$. *Acta Crystallogr*. 1971;27(6): 1245–1252. DOI: https://doi.org/10.1107/s0567740871003819

9. Ohmasa M., Nowacki W. A redetermination on the crystal structure of aikinite (BiS_2/S/S/$Cu^{IV}Pb^{VII}$). *Z. Krystallogr*. 1970;132(1–6): 71–86. DOI: https://doi.org/10.1524/zkri.1970.132.1-6.71

10. Strobel S., Sohleid T. Three structures for strontium copper (I) lanthanidis (III) selinides $SrCuMeSe_3$ (M=La, Gd, Lu). *J. Alloys and Compounds*. 2006;418(1–2): 80–85. DOI: https://doi.org/10.1016/j.jallcom.2005.09.090

11. Sikerina N. V., Andreev O. V. Kristallicheskaya struktura soedinenii $SrLnCuS_3$(Ln=Gd, Lu) [Crystal structure of $SrLnCuS_3$ compounds (Ln = Gd, Lu)]. *Russian Journal of Inorganic Chemistry*. 2007;52(4): 641–644. Available at: https://www.elibrary.ru/item.asp?id=9594111 (In Russ.)

12. Edenharter A., Nowacki W., Takeuchi Y. Verfeinerung der kristallstructur von Bournonit [$(SbS_3)_1$/$Cu_2^{IV}Pb^{VII}Pb^{VIII}$] und von seligmannit [$(AsS_3)_2$/$Cu_2^{IV}Pb^{VII}Pb^{VIII}$]. *Z. Kristallogr*. 1970;131(1): 397–417. DOI: https://doi.org/10.1524/zkri.1970.131.1-6.397

13. Kaplunnik L. N. Kristallicheskie struktury mineralov velikita, aktashita, shvatsita, tennantita, galkhaita, lindstremita-krupkaita i sinteticheskoi Pb, Sn sul'fosoli [The crystal structures of the minerals are granite, actashite, schwa-cit, tennantite, galhaite, lindstromite-krupkaite and synthetic Pb, Sn sulphosols]. *Abstract. diss. cand. geol.-miner. sciences*. Moscow: MSU Publ.; 1978. 25 p. Available

at: https://search.rsl.ru/ru/record/01007805415 (In Russ.)

14. Gasymov V. A., Mamedov H. S. On the crystal chemistry of the intermediate phases of the vis-mutin-aikinite system (Bi_2S_3–$CuPbBiS_3$). *Azerb. khim. zhurn*. [Azerbaijan Chemical Journal]. 1976;(1): 121–125. Available at: https://cyberleninka.ru/article/n/fazovye-ravnovesiya-v-sisteme-pbla2s4-pbbi2s4 (In Russ., abstract in Eng.)

15. Christuk A. E., Wu P., Ibers J. A. New quaternary chalcogenides $BaLnMQ_3$ (Ln – Rare Earth; M = Cu, Ag; Q = S, Se). *J. Solid State Chem*. 1994;110(2): 330–336. DOI: https://doi.org/10.1006/jssc.1994.1176

16. Wu P., Ibers J. A. Synthesis of the new quaternary sulfides $K_2Y_4Sn_2S_{11}$ and $BaLnAgS_3$ (Ln = Er, Y, Gd) and the Structures of $K_2Y_4Sn_2S_{11}$ and $BaErAgS_3$. *J. Solid State* Chem. 1994;110(1): 156–161. DOI: https://doi.org/10.1006/jssc.1994.1150

17. Pobedimskaya E. A., Kaplunnik L. N., Petrova I. V. *Crystal chemistry of sulfides. Results of Science and Technology. Series crystal chemistry*. Moscow: Publishing House of the Academy of Sciences of the USSR; 1983. 17: 164 p. (In Russ.)

18. Gulay L. D., Shemet V. Ya., Olekseyuk I. D. Investigation of the R_2S_3–Cu_2S–PbS (R = Y, Dy, Ho and Er) systems. *J. Alloys and Compounds*. 2007;43(1–2): 77–84. DOI: https://doi.org/10.1016/j.jallcom.2006.05.029

19. Kostov I., Mincheva-Stefanova I. *Sulfide minerals*. Moscow: Mir, 1984. 281 p.

20. Alieva R. A., Bayrmova S. T., Aliev O. M. Phase diagrams of the $CuSbS_2$-MS (M = Pb, Eu, Yb) systems. *Inorganic Materials*. 2010;46 (7): 703–706. DOI: https://doi.org/10.1134/S0020168510070022

21. Bayramova S. T., Bagieva M. R., Aliev O. M., Ragimova V. M. Synthesis and properties of structural analogs of the mineral bournonite. *Inorganic Materials*. 2011;47(4): 345–348. DOI: https://doi.org/10.1134/S0020168511040054

22. Bayramova S. T., Bagieva M. R., Aliev O. M. Phase relations in the $CuAsS_2$–MS (M – Pb, Eu, Yb) systems. *Inorganic Materials*. 2011; 47 (3): 231–234. DOI: https://doi.org/10.1134/S0020168511030046

23. Aliev O. M., Ajdarova D. S., Bayramova S. T., Ragimova V. M. Nonstoichiometry in $PbCuSbS_3$. *Azerb. chem. journal*. 2016;(2): 51–54. Available at: https://cyberleninka.ru/article/n/nonstoichiometry-in-pbcusbs3-compound

24. Aliev O. M., Ajdarova D. S., Agayeva R. M., Ragimova V. M. Phase formation in quasiternary system Cu_2S–PbS–Sb_2S_3. *Intern Journal of Application and Fundamental Research*. 2016;(12): 1482–1488. Available at: https://applied-research.ru/pdf/2016/2016_12_8.pdf (In Russ., abstract in Eng.)

25. Aliev O. M., Azhdarova D. S., Agayeva R. M., Maksudova T. F. Phase relations along the $Cu_2S(Sb_2S_3$, $PbSb_2S_4$, $Pb_5Sb_4S_{11})$–$PbCuSbS_3$ joins in the pseudoternary system Cu_2S–PbS–Sb_2S_3 and physical properties of $(Sb_2S_3)_{1-x}(PbCuSbS_3)_x$ solid solutions. *Inorganic Materials*. 2018;54(12): 1199–1204. DOI: https://doi.org/10.1134/S0020168518120014

26. Rzaguluev V. A., Kerimli O. Sh., Azhdarova D. S., Mammadov Sh. H., Aliev O. M. Phase equilibria in the Ag_8SnS_6–Cu_2SnS_3 and Ag_2SnS_3–$Cu_2Sn_4S_9$ systems. *Kondensirovannye sredy i mezhfaznye granitsy = Condensed Matter and Interphases*. 2019;21 (4): 544–551. DOI: https://doi.org/10.17308/kcmf.2019.21/2365 (In Russ., abstract in Eng.)

Information about the authors

Ozbek M. Aliev, DSc in Chemistry, Professor, M. Nagiyev Institute of Catalysis and Inorganic Chemistry of National Academy of Sciences of Azerbaijan, Baku, Azerbaijan; e-mail: azxim@mail.ru.

Sabina T. Bayramova, PhD in Chemistry, Baku European Lyceum, Baku, Azerbaijan; e-mail: azxim@mail.ru.

Dilbar S. Ajdarova, DSc in Chemistry, Chief Researcher, M. Nagiyev Institute of Catalysis and Inorganic Chemistry of National Academy of Sciences of Azerbaijan, Baku, Azerbaijan; e-mail: azxim@mail.ru.

Valida M. Ragimova, PhD in Chemistry, Assistant Professor, Leading Researcher, M. Nagiyev Institute of Catalysis and Inorganic Chemistry of National Academy of Sciences of Azerbaijan, Baku, Azerbaijan; e-mail: azxim@mail.ru.

Sharafat H. Mammadov, PhD in Chemistry, Assistant Professor, M. Nagiyev Institute of Catalysis and Inorganic Chemistry of National Academy of Sciences of Azerbaijan, Baku, Azerbaijan; e-mail: azxim@mail.ru. ORCID ID: https // orcid.org / 0000-0002-1624-7345.

All authors have read and approved the final manuscript.

Translated by Valentina Mittova
Edited and proofread by Simon Cox